

Phonon dispersion relation in $\text{YBa}_2\text{Cu}_3\text{O}_7$

S. L. Chaplot

Nuclear Physics Division, Bhabha Atomic Research Center, Bombay 400 085, India

(Received 8 September 1987; revised manuscript received 9 February 1988)

The phonon spectrum in $\text{YBa}_2\text{Cu}_3\text{O}_7$ is calculated in the orthorhombic structure using an unscreened rigid-ion model as a first approximation. The calculated values of the "neutron-weighted" phonon density of states, the optical frequencies, the Debye temperature, and the mean-squared vibrational amplitudes are in fair agreement with the values reported from various experiments.

I. INTRODUCTION

The phonon properties of the solid $\text{YBa}_2\text{Cu}_3\text{O}_7$ and related compounds are of importance in establishing whether or not the phonon mechanism is dominant in the superconducting behavior of these compounds at a high T_c of about 90 K. Weber¹ has recently calculated the phonon spectrum and the electron-phonon interaction in the compounds $\text{La}_{2-x}(\text{Ba},\text{Sr})_x\text{CuO}_4$ and shown that the T_c of about 35 K in these systems is caused by a large electron-phonon coupling. Doubts have been expressed in the literature about whether the phonon mechanism itself could result in the higher T_c of about 90 K in $\text{YBa}_2\text{Cu}_3\text{O}_7$, etc., and other mechanisms of superconductivity have been proposed.^{2,3} Precise numerical calculations in the various mechanisms are therefore necessary. In this paper we present a calculation of the detailed phonon spectrum and related properties in $\text{YBa}_2\text{Cu}_3\text{O}_7$.

The calculation by Weber¹ on $\text{La}_{2-x}(\text{Ba},\text{Sr})_x\text{CuO}_4$ was carried out in the framework of the nonorthogonal tight-binding theory of lattice dynamics in which the phonon dynamical matrix is divided into two contributions, one representing the "bare" phonon frequencies, and other renormalization due to the conduction electrons. The latter essentially gave rise to large Kohn anomalies near the Brillouin-zone boundary involving certain oxygen-bond-stretching vibrations of the breathing type. The bare phonon part, which provided the unrenormalized phonon spectrum, was obtained from a Born-von Karman force-constant model which was derived from a similar model for $\text{Ba}(\text{Pb-Bi})\text{O}_3$ with changes in certain force constants. It was recognized that the magnitude of the $\text{Cu-O}(2)$ force constant was of great importance.

Most of the compounds of the type $\text{YBa}_2\text{Cu}_3\text{O}_x$ ($x=6$ to 7), except for the high- T_c superconductor (x about 7), are believed to be either ionic insulators or semiconductors. From the similarity of the observed crystal structures of all these compounds, it may be suggested that the interatomic interactions in them may be quite similar, except that in the metallic (x about 7) compound the long-range ionic interaction should be screened. Although there are also the metallic and weak covalent contributions to the crystal binding, the dominant contribution to the binding energy arises from the Coulomb interaction between the negative and positive ions, even when it is screened in the long range.

Recently Sugai⁴ has reported significant LO-TO phonon-frequencies splitting for certain phonons as determined from their observed far-infrared reflection spectrum of $\text{YBa}_2\text{Cu}_3\text{O}_7$, and has suggested that the long-range interaction in this solid may be screened only partly and anisotropically.

It may also be noted that in this solid the carrier density and the conductivity (above T_c) are much smaller than that in the well-known metals like copper. In view of this, in the lattice-dynamical model for this solid, as a first approximation, we have considered an unscreened potential. The model calculation thus provides only the "bare" phonon frequencies. The immediate motivation was to calculate several of the properties which have been observed experimentally,⁴⁻⁹ and which are perhaps not much influenced by the screening, namely, the total phonon density of states, mean-square atomic vibrational amplitudes, Debye temperature, etc. Experimental values of these above properties have agreed well with the results of the calculations. Even the optical-phonon frequencies, as determined by Raman scattering and the infrared reflection spectrum, are in encouraging agreement with our approximate calculation.

The calculation has also produced phonon eigenvectors which may be used as a guide in the assignment of the optical frequencies, and also in planning comprehensive inelastic neutron scattering experiments. Once sufficient experimental data on the dynamics become available, the model may be improved by fitting to those data, and also the \mathbf{q} -dependent anisotropic screening may be incorporated in the model. It is believed that except for the dispersion of the "sensitive" phonon branches, many of the qualitative features in the phonon density of states will not be altered significantly.

For the requirements of consistency, the present lattice dynamical model has used the condition of overall charge neutrality of the unscreened effective ionic charges, and the stability of the structure. The calculated force constants and the phonon frequencies in the model should be considered as correct to a first approximation in view of the fair agreement of the calculated results with many of the experiments as shown in the paper. Such first-approximation calculations are necessary for complex structures like $\text{YBa}_2\text{Cu}_3\text{O}_7$ for a quick contact with experiments, whereas more accurate calculations will take much more effort.

TABLE I. Interatomic potential parameters in the rigid-ion model of $\text{YBa}_2\text{Cu}_3\text{O}_7$. The labeling of atoms is as per Ref. 9(a).

	Y	Ba	Cu(1)	Cu(2)	O(1)	O(2)	O(3)	O(4)
Z	2.1	1.5	1.2	1.4	-1.05	-1.4	-1.4	-1.4
R (nm)	0.183	0.233	0.116	0.120	0.155	0.174	0.174	0.177

It may also be pointed out that the present work is perhaps the only reported lattice-dynamical calculation on $\text{YBa}_2\text{Cu}_3\text{O}_7$ other than the short-range force-constant model of Stavola *et al.*⁶ While the latter model has utilized the experimental optical frequencies for getting the values of the force constants, the present model parameters have been instead obtained from the stability conditions of the structure and have produced a phonon density of states in a better agreement with the experimental data. Stavola *et al.* have, however, not given further details of their results which could be compared with the present work. The present work on $\text{YBa}_2\text{Cu}_3\text{O}_7$ has been briefly reported in some of the national symposia.¹⁰

It may also be noted for completeness that Prade *et al.*⁶ have reported lattice-dynamical calculations for $\text{La}_{2-x}\text{M}_x\text{CuO}_4$ using an unscreened shell model. The calculated phonon frequencies were in a reasonable agreement with those available from the Raman and infrared experiments. The calculated LO-TO splittings would be quenched, at least partly or anisotropically, when the screening is considered.

II. THEORETICAL MODEL

Our purpose of this paper is to provide an improved model for the bare phonon frequencies in $\text{YBa}_2\text{Cu}_3\text{O}_7$, in particular, by using an interatomic potential function rather than the numerous force constants as parameters and also by using a potential which is consistent with the requirements of the static and dynamic stability of the crystal structure.

In view of the considerations given earlier in the paper, we have adopted an unscreened rigid-ion model in which the ions are considered as rigid (unpolarizable) during vibrations. The shell model, which allows polarization of ions, is not used here as it involves several additional parameters which cannot be meaningfully obtained with the limited experimental data available so far. The present model has been used successfully earlier for the perovskite KNbO_3 and many other systems,¹¹ which, however, do not involve screening. Pair-wise atom-atom interactions consisting of the Coulombic potential and the Born-Mayer-type short-range repulsive potential are used. The

TABLE II. The experimental and calculated structure and thermal parameters of $\text{YBa}_2\text{Cu}_3\text{O}_7$. The labeling of atoms is as per Ref. 9(a).

	Calculated	X-ray ^a	X-ray ^b	Neutron ^c	Neutron ^d
a (nm)	0.384	0.3856	0.3827	0.3819	0.3810
b (nm)	0.393	0.3870	0.3877	0.3883	0.3883
c (nm)	1.107	1.1666	1.1708	1.1664	1.1674
Fractional Z coordinates					
Ba	0.191	0.1862	0.1873	0.1844	0.1841
Cu(2)	0.354	0.3572	0.3558	0.3554	0.3550
O(1)	0.168	0.153	0.155	0.1579	0.1584
O(2)	0.380	0.380	0.3807	0.3788	0.3778
O(3)	0.380	0.379	0.3807	0.3771	0.3780
Isotropic temperature factors at 300 K $B = (8\pi^2/3)[\langle u^2(x) \rangle + \langle u^2(y) \rangle + \langle u^2(z) \rangle]$ (\AA^2)					
Y	0.5	0.5	0.7	0.9	0.5
Ba	0.6	0.8	0.5	0.8	0.6
Cu(1)	0.8	1.1	0.9	0.9	0.4
Cu(2)	0.8	0.7	0.5	0.6	0.4
O(1)	1.6	1.3	1.6	0.8	0.8
O(2)	0.8	0.4	0.2	0.3	0.7
O(3)	0.8	1.2	0.2	0.6	0.4
O(4)	1.8	2.0	4.2	2.9	1.8
Anisotropic B					
O(4) XX	2.9			4.8	1.8
YY	1.5			1.4	(=1.8)
ZZ	1.0			2.5	0.8

^aReference 9(a).

^bReference 9(b).

^cReference 9(c).

^dReference 9(d).

effect of polarization of ions is partly included by assuming adjustable effective charges on ions. The crystal potential energy is taken as consisting of two-body potentials between different atoms k and k' separated by a distance r , as given by

$$V(r) = (e^2/4\pi\epsilon_0)Z(k)Z(k')/r + a \exp\{-br/[R(k)+R(k')]\},$$

with $e^2/4\pi\epsilon_0 = 14.4 \text{ eV/\AA}$, $a = 1822 \text{ eV}$, and $b = 12.364$. Here $Z(k)$, $Z(k')$ are the "effective" charges situated at

the ionic positions. In the unscreened rigid-ion model, the charge neutrality of the unit cell is maintained. The $R(k)$, $R(k')$ are referred to as "effective radii" and are treated as adjustable parameters along with the effective charges. The parameters $R(k)$ turn out to be nearly proportional to the crystal radii of atoms. The coefficient a is assumed to be a constant as in our earlier studies.¹¹ The constant b which could be contained in $R(k)$ itself, is chosen only for convenience.

The calculation on $\text{YBa}_2\text{Cu}_3\text{O}_7$ has been made in the orthorhombic structure of the space group $Pmmm$ as determined by x-ray diffraction⁹ with the oxygen atom at $(0,0.5,0)$ having full occupancy. Through systematic variation of the parameters we have obtained a set of values which provide the static and dynamic stability of the structure. In particular, it is ensured that the total potential is at a minimum with respect to the lattice constants and the atomic positional coordinates, and the eigenvalues $[\omega^2(\mathbf{q}j)]$ are positive for all the wave vectors (\mathbf{q}) in the Brillouin zone and all the branches (j) of the dispersion relation. In the potential minimization procedure, the space-group symmetry is not altered but the lattice constants and the positional coordinates are slightly changed to conform to the exact minimum.

The potential parameters as obtained by the above procedure are given in Table I. The charge parameters are only a fraction of the full ionic charges, which is similar to the case of KNbO_3 (Ref. 11). Slightly different parameters are required from the stability conditions for the atoms which are not related by symmetry. These parameters have not been fitted to any experimental phonon results since sufficient data are not available, except that it is ensured that the maximum of the phonon frequencies is approximately of the right magnitude. The above potential parameters produce a minimum for the structure as given in Table II, which is in good agreement with the observed structure⁹ except that the model gives a somewhat larger $\text{Cu}(1)-\text{O}(1)$ bond length.

III. RESULTS AND DISCUSSION

Figure 1(a) gives the calculated spectrum of the phonon frequencies. For comparison with the inelastic neutron scattering data, we give in Fig. 1(b), the "neutron-weighted" density of states in which the contributions

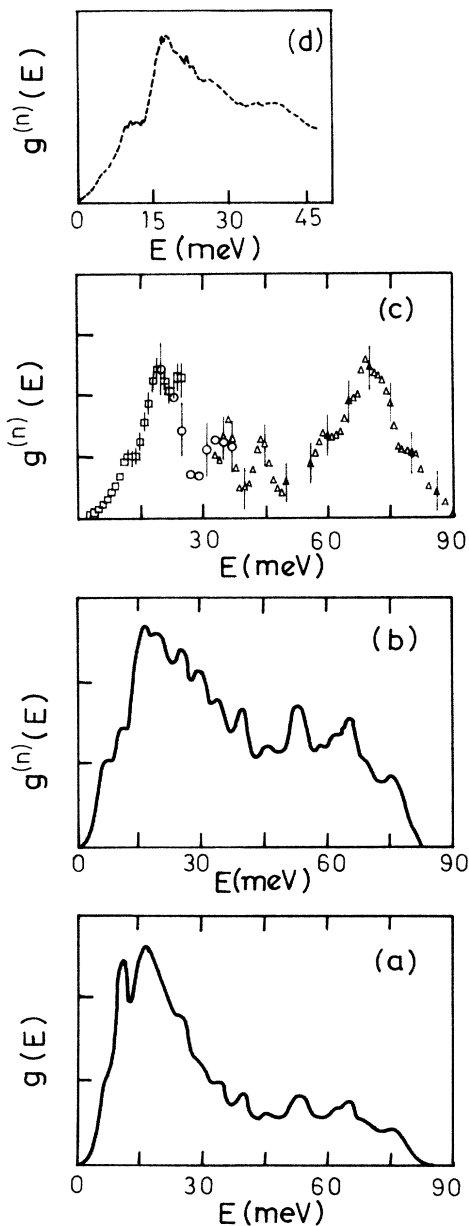


FIG. 1. (a) The calculated spectrum of the "bare" phonon frequencies. (b) The calculated "neutron-weighted" density of states. The experimental spectrum corresponding to (b) as obtained from inelastic neutron scattering is given in (c) from Rhyne *et al.* (Ref. 7) (at 120 K), and (d) from Mihály *et al.* (Ref. 7) (at 300 K).

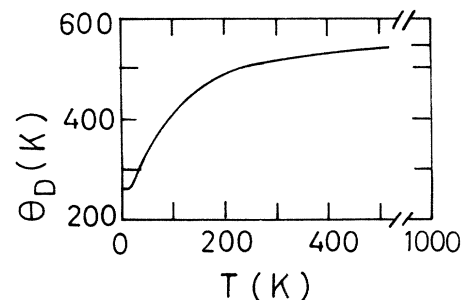


FIG. 2. The calculated Debye temperature $\theta_D(T)$ as a function of temperature T .

from the different atomic species have been multiplied by their neutron-scattering-weightage factor. This factor ($4\pi b^2/m$, b = scattering length, m = mass), for the atomic species Y, Ba, Cu, and O is, respectively, 0.0849, 0.0252, 0.1178, and 0.2647 barns/amu; the largest being for the oxygens. In both the Figs. 1(a) and 1(b), we have included smoothening of the spectra with Gaussians of the full

width at half maximum of 2 meV. Figures 1(c) and 1(d), respectively, give the reported neutron spectra of Rhyne *et al.*⁷ and Mihály *et al.*⁷ The agreement between the calculated and the experimental spectra is excellent in spite of the fact that the calculated spectrum refers to "bare" phonon frequencies only. (One of the reasons may be that the screening affects only a few phonons.) The low-energy re-

TABLE III. Experimental and calculated optical-phonon frequencies in $\text{YBa}_2\text{Cu}_3\text{O}_7$ at the Brillouin-zone center.

Raman-active phonon frequencies (cm^{-1}) ^a									
Experimental results									
Ref. 5(a)	Ref. 5(i)	Ref. 5(j)	Ref. 5(h)	Ref. 5(f)	Ref. 5(g)	Ref. 5(b)	Ref. 5(c)	Ref. 5(d)	Ref. 5(e)
142 (A_g)	225	430	435	432	155	337	340	140 (A_g)	339
338	339	497	495	505	175	440	436	230 (A_g)	432
483 (A_g)	427	583			295	502	504	335 (A_g)	499
595 (A_g)	500	632			335		640	435 (A_g)	588
	580				440			500 (A_g)	641
	637				509				
					581				
					638				
Calculated results									
			A_g	B_{3g}	B_{2g}				
			114	61	48				
			142	120	126				
			317	211	234				
			348	326	268				
			633	492	498				
Infrared-active phonon frequencies (cm^{-1})									
Experimental results									
	Ref. 4(c)		Refs. 4(a) and 4(e)	Ref. 4(d)	Ref. 4(f)		Ref. 4(b)		
	LO	TO					TO	LO	
	128	149	151	151	153		103	145	
	182	195	191	268	193		158	233	
	232	284	279	303	270		201		
	302	316	310		310		275		
	388	474	548		480		311		
	489	510	609		575				
	527	574							
	596	618							
	641								
	691								
Calculated results									
		B_{1u}		B_{2u}		B_{3u}			
	LO	TO	LO	TO	LO	TO			
	86	66	84	84	28	16			
	97	92	137	135	96	94			
	140	137	179	170	159	159			
	208	145	257	223	194	182			
	347	208	414	276	270	269			
	499	427	526	415	528	280			
	622	550	559	527	572	529			

^aThe Raman mode at about 640 cm^{-1} has been suggested to be not at the zone center, but instead, induced by disorder scattering.

TABLE IV. Results of the calculation of the phonon frequencies and eigenvectors at the Brillouin-zone center. For the orthorhombic structure of $\text{YBa}_2\text{Cu}_3\text{O}_7$, each of the group-theoretical representations involve vibrations only along one direction as indicated below. The labeling of the atoms is as given by Siegrist *et al.* (Ref. 9). The eigenvector components (root mass multiplied by displacements) are given for the atoms in the asymmetric cell ($0 \leq z \leq 0.5$). For the remaining atoms ($z < 0$) the displacements are opposite to their related atoms in the asymmetric cell for the representations A_g , B_{2g} , and B_{3g} , and are the same for the representation B_{1u} , B_{2u} , and B_{3u} . The first column gives, respectively, the representation, the direction of vibrational displacements, and the components of the polarizability tensor α and the dipole moment vector T . LO and TO refer to the longitudinal and transverse optic phonons. The splitting between the LO and TO modes would be quenched anisotropically if screening of the macroscopic field were included in the dynamical model.

Representation	Frequency ν (cm^{-1})		Eigenvector components							
	LO	TO	Y	Ba	Cu(1)	Cu(2)	O(1)	O(2)	O(3)	O(4)
A_g, z, α_{xx}	114	$-\nu(\text{LO})$	0	96	0	0	28	5	4	0
a_{yy}, α_{zz}	142	...	0	-1	0	96	-4	22	19	0
	317	...	0	2	0	3	-6	-71	70	0
	348	...	0	-28	0	4	96	-5	3	0
	633	...	0	-6	0	-29	0	67	68	0
B_{3g}, y, α_{yz}	61	...	0	80	0	45	13	29	26	0
	120	...	0	-60	0	56	0	44	37	0
	211	...	0	5	0	-69	-4	47	54	0
	326	...	0	-10	0	-8	98	-10	6	0
	492	...	0	0	0	8	-11	-70	70	0
B_{2g}, x, α_{zx}	48	...	0	81	0	42	26	22	23	0
	126	...	0	-55	0	65	4	34	39	0
	234	...	0	-20	0	-4	95	-10	-22	0
	268	...	0	-2	0	-63	15	51	57	0
	498	...	0	0	0	1	-7	76	-65	0
B_{1u}, z, T_z	...	66	-23	18	33	-66	53	0	-4	29
	86	...	-17	33	38	-59	18	-53	19	15
	...	92	3	10	6	-8	-10	-76	62	-2
	97	...	15	-19	-24	32	-12	-51	71	-8
	...	137	-2	-70	36	33	31	13	33	22
	140	...	-10	-54	77	27	-2	0	3	17
	...	145	13	-1	-77	-7	47	18	36	2
	208	...	85	-26	8	-44	-5	12	5	-1
	...	208	85	-22	12	-43	-15	8	1	-3
	347	...	1	-25	-13	4	95	-1	0	-14
	...	427	13	-5	13	13	53	-27	-26	-72
	499	...	1	-11	-29	1	7	0	-2	95
	...	550	-24	6	20	-24	-19	49	50	-56
622	...	30	6	0	30	-1	-63	-64	-1	
B_{2u}, y, T_y	...	84	-63	52	31	-35	12	-20	-21	12
	84	...	-64	51	31	-36	13	-18	-19	13
	...	135	8	-51	79	-5	20	-3	0	24
	137	...	-16	49	-80	6	-18	10	6	-22
	...	170	-67	-20	-3	57	5	36	21	1
	179	...	-61	-23	7	74	-1	15	-2	-3
	...	223	-3	2	2	-58	-3	54	61	-1
	257	...	11	-5	-36	20	56	-42	-38	43
	...	276	1	-10	-42	-9	71	-6	3	54
	414	...	-2	-4	4	-5	66	-4	11	-74
	...	415	-1	-3	6	-2	62	-8	6	-78
	526	...	12	3	3	-4	3	59	-78	-12
	...	527	-8	0	0	10	-10	-69	70	4
	559	...	20	17	19	28	-40	-59	-37	-41

Table IV. (Continued)

Representation	Frequency ν (cm^{-1})		Y	Ba	Cu(1)	Eigenvector components				
	LO	TO				Cu(2)	O(1)	O(2)	O(3)	O(4)
B_{3u}, x, T_x	...	16	19	1	-48	21	25	11	10	-78
	28	...	19	-5	-49	23	26	16	16	-74
	...	94	58	-65	-1	31	-18	17	18	22
	96	...	62	-63	4	28	-23	12	12	24
	...	159	18	37	-71	-7	-46	-2	-1	32
	159	...	13	37	-73	-4	-45	1	3	33
	...	182	-67	-12	-19	59	-6	19	30	16
	194	...	-62	-14	-5	73	-19	4	16	9
	...	269	4	-11	-35	5	77	-15	-26	43
	270	...	5	-10	-30	23	65	-31	-42	37
	...	280	-5	-3	-9	-56	23	54	57	12
	528	...	-3	2	3	7	-11	68	-72	-5
	...	529	-6	0	1	3	-6	75	-66	-1
	572	...	21	17	17	30	-39	-59	-45	-34

gions of the spectra are in a better agreement than the higher energy regions. Most peak positions agree although the energy resolution in the experiments does not resolve many peaks. The peak heights should be compared with caution since the experimental peak heights may not represent the true density of states to the extent that the wave-vector transfer Q has not been completely averaged.

We also calculated the partial density of states separately from the contributions of the different atoms and with different polarizations. These were used in calculating the mean-squared vibrational amplitudes and so the thermal parameters, for comparison with the corresponding values obtained from diffraction experiments. The calculated isotropic temperature factors for the various atoms at 300 K are also given in Table II and can be seen to be in fair agreement with the values obtained from the x-ray- and neutron-diffraction experiments.

The total phonon density of states is used in calculating the lattice contribution to the specific heat as a function of temperature. These values may be related to an effective Debye temperature at each temperature. The calculated Debye temperature so obtained as a function of temperature is plotted in Fig. 2, which shows considerable variation. This, however, is only the reflection of the fact that, in complex systems, the density of states cannot be approximated to a Debye spectrum. The value of the Debye temperature found from the measured specific heat⁸ is nearly 400 to 440 K near T_c (about 90 K) and it corresponds well with the calculated value of 400 K in Fig. 2.

The calculated phonon frequencies at the Brillouin-zone center are given in Table III and compared with the available data from Raman⁵ and infrared⁴ experiments. The experimental⁴ infrared active TO and LO modes were given by the peaks in the $\text{Im}(\epsilon)$ and $-\text{Im}(1/\epsilon)$, respectively, which were obtained from the Kramers-Kronig transformation of the observed far-infrared reflection spectra. At least a part of the LO-TO splitting in the

present calculations will be quenched when (anisotropic) screening is considered. There is generally a fair agreement of the calculations with the observed modes. Detailed comparison at this stage is difficult in view of the differences among the experimental data from the different sources, and also since most of the data have not been classified by group theory. Moreover, only a small number of the expected optical phonons have been observed in the experiments.

Table IV gives the calculated eigenvectors. The group theoretical classification is carried out for the orthorhombic structure of $\text{YBa}_2\text{Cu}_3\text{O}_7$ in the space group $Pmmm$. It turns out that the modes of representations A_u and B_{1g} do not occur for this crystal structure. Raman and infrared activity of the various modes is indicated in Table IV.

Figure 3 gives the calculated phonon dispersion relation for the wave vectors along four different symmetry directions a^* , b^* , c^* , and a^*+b^* . There is considerable dispersion of most of the branches, except those having their wave vectors along the direction c^* . There is one particularly low frequency (soft) branch along c^* which corresponds to the motion of O(4) atoms along the a direction. Softening of this mode would destabilize the one-dimensional ordered Cu(1)-O(4) arrangement along the b direction. It is natural to expect that the position of the O(4) atoms would have significant effect on this particular mode. In this context, the relative stability of the orthorhombic and the tetragonal structures can be studied by comparing their Gibbs free energies as a function of temperature as in our recent study on tetracyanoethylene.¹²

It is evident from the calculated eigenvectors that the high-frequency modes essentially involve only the oxygen atoms, as may be expected due to their smaller mass. Intermediate frequency modes generally involve motions of different atoms. However, if large renormalization occurs for some of the high-frequency phonons, due to their coupling with the electrons, the renormalized phonon

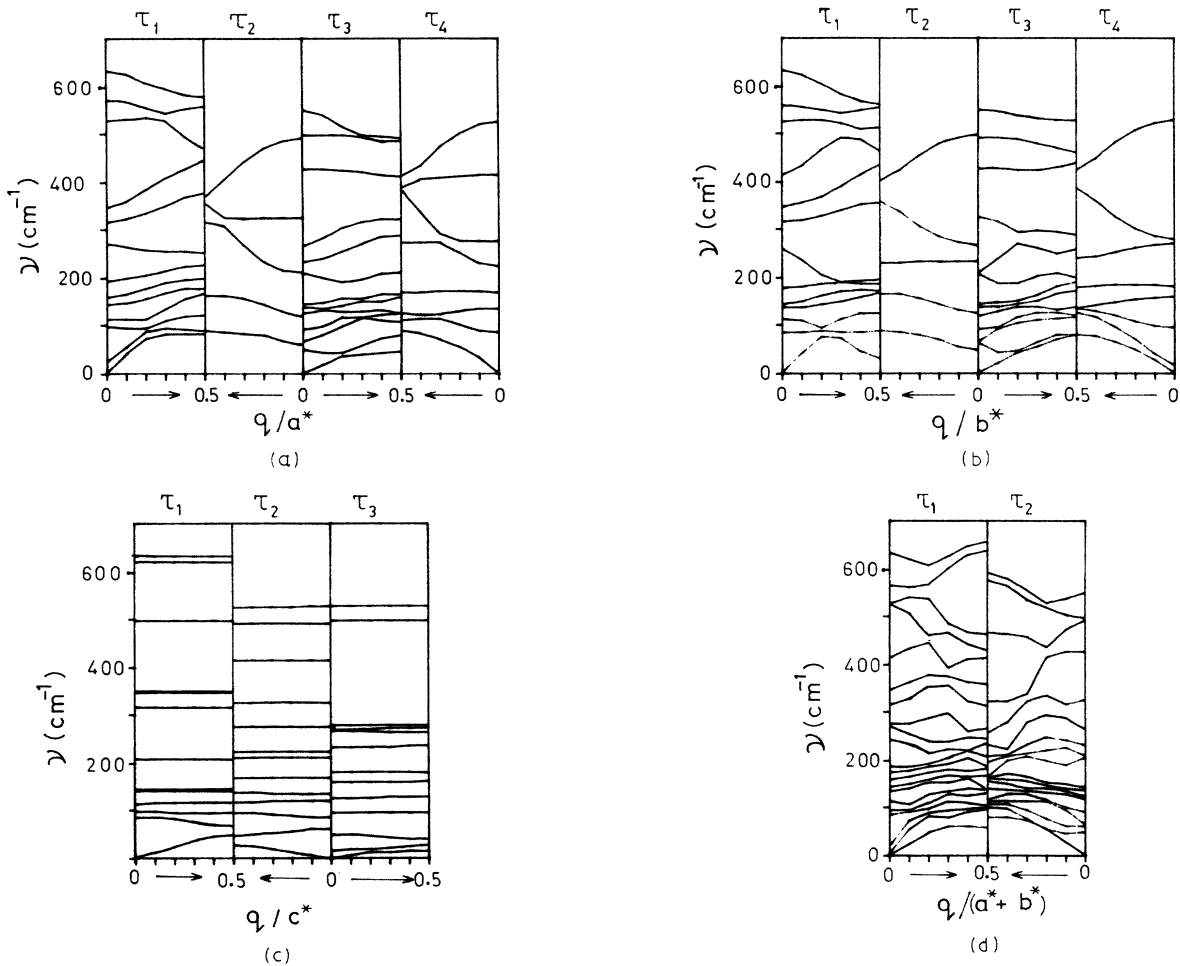


FIG. 3. The calculated phonon dispersion relation for $\text{YBa}_2\text{Cu}_3\text{O}_7$ in the rigid-ion model, for wave vectors along the directions (a) a^* , (b) b^* , (c) c^* , and (d) a^*+b^* .

branches would anticross with other low-frequency branches and therefore have significantly mixed character in terms of the involvement of different atoms in these phonons. The above discussion is particularly relevant since the significantly renormalized phonons are the ones that will significantly enter the phonon mechanism of superconductivity. When such phonons involve more than one species of atoms, a suitable effective mass would enter in the analysis of the isotope effect.¹³

It may be expected¹ that only a few of the oxygen phonons in limited regions of the Brillouin zone (BZ) interact significantly with the conduction electrons, and significantly renormalize in frequencies. Such phonons would constitute only a small part of the total phonon spectrum, and due to their renormalization, have frequencies somewhere in the middle of the total frequency range. One may recall that the neutron inelastic spectrum as observed from a polycrystalline sample has contributions from all the phonon modes. It would therefore be desirable to study individual phonons, through proper selection rules, by using a single crystal in the neutron inelastic scattering. Such phonon selection rules can be obtained from the calculated phonon eigenvectors.

In this paper we have provided an unscreened rigid-ion

model for the bare phonon spectrum in $\text{YBa}_2\text{Cu}_3\text{O}_7$ based on a reasonable interatomic potential which is also consistent with the stability of the crystal structure. The results bring out the general features of the energy spectrum of the phonon modes and also the details of the participation of different atoms in different modes as evident from the calculated eigenvectors. While the calculated overall phonon spectrum and many of the related properties agree well with the experimental results, the model may be improved by incorporating in it the effects of screening. The potential function model would be suitable to derive and compare the structural and phonon properties of related compounds and related crystal structures involving slightly different interatomic separations. Such a model can also be applied in conditions where the harmonic approximation does not hold good, namely at finite temperatures and pressures using, say, the molecular-dynamics computer simulations.

ACKNOWLEDGMENT

The author wishes to thank V. C. Sahni for useful discussion and K. R. Rao for his kind encouragement.

- ¹W. Weber, Phys. Rev. Lett. **58**, 1371 (1987); **58**, 2154(E) (1987).
- ²P. W. Anderson, G. Baskaran, Z. Zou, and T. Hsu, Phys. Rev. Lett. **58**, 2790 (1987), and references therein.
- ³V. J. Emery, Phys. Rev. Lett. **58**, 2794 (1987), and references therein.
- ⁴(a) D. A. Bonn, J. E. Greedan, C. V. Stager, T. Timusk, M. G. Doss, S. L. Herr, K. Kamáras, and D. B. Tanner, Phys. Rev. Lett. **58**, 2249 (1987); (b) S. Perkowitz, G. L. Carr, B. Lou, S. S. Yom, R. Sudharsanan, and D. S. Ginley, Solid State Commun. **64**, 721 (1987); (c) S. Sugai, Phys. Rev. B **36**, 7133 (1987); (d) G. A. Thomas, H. K. Ng, A. J. Millis, R. N. Bhatt, R. J. Cava, E. I. Rietman, D. W. Johnson, Jr., G. P. Espinosa, and J. M. Vandenberg, Phys. Rev. B **36**, 846 (1987); (e) K. Kamáras, C. D. Porter, M. G. Doss, S. L. Herr, D. B. Tanner, D. A. Bonn, J. E. Greedan, A. H. O'Reilly, C. V. Stager, and T. Timusk, Phys. Rev. Lett. **59**, 919 (1987); (f) M. Cardona, L. Genzel, R. Liu, A. Wittlin, Hj. Mattausch, F. García-Alvarado, and E. García-González, Solid State Commun. **64**, 727 (1987).
- ⁵(a) R. J. Hemley and H. K. Mao, Phys. Rev. Lett. **58**, 2340 (1987); (b) P. B. Kirby, M. R. Harrison, W. G. Freeman, I. Samuel, and M. J. Haines, Phys. Rev. B **36**, 8315 (1987); (c) G. A. Kourouklis, A. Jayaraman, B. Batlogg, R. J. Cava, M. Stavola, D. M. Krol, E. A. Rietman, and L. F. Schneemeyer, *ibid.* **36**, 8320 (1987); (d) D. M. Krol, M. Stavola, W. Weber, L. F. Schneemeyer, J. V. Waszczak, S. M. Zahurak, and S. G. Kosinski, *ibid.* **36**, 8325 (1987); (e) S. Blumenröder, E. Zirngieble, H. Schmidt, G. Güntherodt, and H. Brenten, Solid State Commun. **64**, 1229 (1987); (f) R. Liu, R. Merlin, M. Cardona, H. Mattausch, W. Bauhofer, A. Simon, F. García-Alvarado, E. Moran, M. Vallet, J. M. González-Calbet, and M. A. Alario, *ibid.* **63**, 839 (1987); (g) M. Cardona, L. Genzel, R. Liu, A. Wittlin, Hj. Mattausch, F. García-Alvarado, and E. García-González, Solid State Commun. **64**, 727 (1987); (h) M. Stavola, D. M. Krol, W. Weber, S. A. Sunshine, A. Jayaraman, G. A. Kourouklis, R. J. Cava, and E. A. Rietman, Phys. Rev. B **36**, 850 (1987); (i) A. Yamanaka, F. Minami, K. Watanabe, K. Inoue, S. Takekawa, and N. Iyi, Jpn. J. Appl. Phys. **26**, L1404 (1987); (j) Z. Iqbal, S. W. Steinhauser, A. Bose, N. Cipollini, and H. Eckhardt, Phys. Rev. B **36**, 2283 (1987).
- ⁶M. Stavola, D. M. Krol, W. Weber, S. A. Sunshine, A. Jayaraman, G. A. Kourouklis, R. J. Cava, and E. A. Rietman, Phys. Rev. B **36**, 850 (1987); J. Prade, A. D. Kulkarni, F. W. de Wette, W. Kress, M. Cardona, R. Reiger, and U. Schröder, Solid State Commun. **64**, 1267 (1987).
- ⁷L. Mihály, L. Rosta, G. Coddens, F. Mezei, Gy. Hutiray, G. Kriza, and B. Keszei, Phys. Rev. B **36**, 7137 (1987); J. J. Rhyne, D. A. Neumann, J. A. Gotaas, F. Beech, L. Toth, S. Lawrence, S. Wolf, M. Osofsky, and D. U. Gubser, *ibid.* **36**, 2294 (1987).
- ⁸S. E. Inderhees, M. B. Salamon, T. A. Friedmann, and D. M. Ginsberg, Phys. Rev. B **36**, 2401 (1987); M. V. Nevitt, G. W. Crabtree, and T. E. Klippert, *ibid.* **36**, 2398 (1987).
- ⁹(a) T. Siegrist, S. Sunshine, D. W. Murphy, R. J. Cava, and S. M. Zahurak, Phys. Rev. B **35**, 7137 (1987); (b) Y. Le Page, W. R. McKinnon, J. M. Tarascon, L. H. Greene, G. W. Hull, and D. M. Hwang, *ibid.* **35**, 7245 (1987); (c) W. I. F. David, W. T. A. Harrison, J. M. F. Gunn, O. Moze, A. K. Soper, P. Day, J. D. Jorgensen, D. G. Hinks, M. A. Beno, L. Soderholm, D. W. Capone II, I. K. Schuller, C. U. Segre, K. Zhang, and J. D. Grace, Nature **327**, 310 (1987); (d) H. You, R. K. McMullan, J. D. Axe, D. E. Cox, J. Z. Liu, G. W. Crabtree, and D. J. Lam, Solid State Commun. **64**, 739 (1987).
- ¹⁰S. L. Chaplot, in Proceedings of the Workshop on the Theoretical Aspects of the High T_c Superconductors, Bombay, 1987 (unpublished); S. L. Chaplot, Proc. Solid State Phys. Symp. (India) **30C**, 187 (1987).
- ¹¹S. L. Chaplot and K. R. Rao, J. Phys. C **16**, 3045 (1983); S. L. Chaplot, Bhabha Atomic Research Centre, Bombay, Report No. BARC-972, 1978 (unpublished); S. L. Chaplot and V. C. Sahni, Phys. Status Solidi B **96**, 575 (1979).
- ¹²S. L. Chaplot, Phys. Rev. B **36**, 8471 (1987).
- ¹³B. Batlogg, R. J. Cava, A. Jayaraman, R. B. van Dover, G. A. Kourouklis, S. Sunshine, D. W. Murphy, L. W. Rupp, H. S. Chen, A. White, K. T. Short, A. M. Muzsca, and E. A. Rietman, Phys. Rev. Lett. **58**, 2333 (1987); L. C. Bourne, M. F. Crommie, A. Zettle, H.-C. Loye, S. W. Keller, K. L. Leary, A. M. Stacy, K. J. Chang, M. L. Cohen, and D. E. Morris, *ibid.* **58**, 2337 (1987).